

Effect of Solution pH on the Photo-Oxidation of 4-Chlorophenol by Synthesized Silver-Zinc Oxide Photocatalyst

Nur Syafiq Hazirah Razali¹, Hayati Mohamad Mukhair², Kian Mun Lee³, Mohd Izham Saiman¹, and Abdul Halim Abdullah^{1,2*}

¹Department of Chemistry, Faculty of Science, Universiti Putra Malaysia, 43300 UPM Serdang, Selangor Malaysia

²Institute of Nanoscience and Nanotechnology, Universiti Putra Malaysia, 43400 UPM Serdang, Selangor, Malaysia

³Nanotechnology and Catalysis Research Centre (NANOCAT), University of Malaya, 50603 Kuala Lumpur, Malaysia

* **Corresponding author:**

tel: +603-97696777

email: halim@upm.edu.my

Received: January 4, 2022

Accepted: April 11, 2022

DOI: 10.22146/ijc.71763

Abstract: Due to its toxicity, 4-chlorophenol (4CP) must be removed from the wastewater before discharging into open water. In this work, ZnO and Ag-ZnO photocatalysts were prepared via a solvothermal method under mild conditions (150 °C), followed by calcination at 300 °C and then characterized. The addition of Ag resulted in a change of the ZnO morphologies, which exhibited wurtzite structure, from irregular to rod-like shape, lower bandgap energy, and a lower electron-hole recombination rate. The 0.6 Ag-ZnO catalyst showed the highest efficiency in the photooxidation of 4CP under UV irradiation. Molecular 4CP exists in acidic and near-neutral conditions (pH 4 and 6) and is stable towards UV irradiation. Photooxidation of 2.3×10^{-4} mol/L 4CP by 0.8 g of 0.6% Ag-ZnO resulted in 67% removal of molecular 4CP at pH 6 with a rate constant of $4.0 \times 10^{-3} \text{ min}^{-1}$. Under similar conditions, a complete photooxidation of the anionic 4CP was observed at pH 11 with a rate constant of $1.4 \times 10^{-2} \text{ min}^{-1}$. The holes and superoxide radicals are the species responsible for molecular 4CP photooxidation, while hydroxyl radicals are the dominant species for anionic 4CP. The prepared Ag/ZnO photocatalyst exhibit good potential to efficiently oxidize 4CP in both acidic and alkaline conditions.

Keywords: Ag-ZnO; photooxidation; 4-chlorophenol; endocrine disruptor chemicals; photocatalyst

■ INTRODUCTION

Semiconductor photocatalysis has been extensively studied to degrade non-biodegradable and highly persistent pollutants [1]. In principle, when a semiconductor photocatalyst absorbs light energy greater than or equal to its bandgap energy, it produces electron-hole pairs, which generate free radicals through a series of reactions. These free radicals are responsible for degrading organic pollutants to harmless by-products such as H₂O and CO₂ [2]. TiO₂, ZnO, CdS, CeO₂, GaN, WO₃, and ZnS, are the most frequently used semiconductors. Although TiO₂ is the most widely studied photocatalyst, several studies have reported that it has exhibited a significantly lower degradation rate than ZnO since the latter has higher light absorption efficiency

over a significant fraction of the solar spectrum [2-4]. However, the efficiency of ZnO is low due to its fast electron-hole recombination rate.

To suppress the recombination rate and enhance the photocatalytic activity, several researchers have modified the surface of ZnO via doping with C₃N₄, silver, gold, copper, and cobalt [5-9]. The photocatalytic activity of the doped ZnO was superior to pure ZnO due to the lower electron-hole recombination rate [10]. Silver, Ag, one of the best dopants for ZnO, can act as an electron sink, reducing the recombination rate and improving the photocatalyst's performance [11].

Various methods, including sol-gel [12-13], hydrothermal [14-15], co-precipitation [16-18], and thermal treatment [19], have been used to prepare Ag-

ZnO photocatalysts. Although the Ag-ZnO performance, under various reaction conditions, has been widely evaluated via photodegradation of dyes [20], reports on the degradation of chlorophenols by Ag-ZnO are limited. Chlorophenols are toxic and recalcitrant compounds harmful to human health and aquatic life [21]. The production of chlorophenol compounds has increased recently with the worldwide increase in industrial and agricultural activities. They are widely used to produce insecticides, pesticides, and wood preservatives. Their presence has been detected in soils, groundwater [1], and industrial wastewater [3]. 4CP, a known endocrine disruptor chemical, is widely used in manufacturing [2,22]. Due to its toxicity and non-biodegradable, removing 4CP from the wastewater is imperative. Recently, the removal of 4CP via photocatalysis using ZnO/ZnS/ carbon xerogel [23] and CuO-ZnO-PANI [24] was reported. In this study, ZnO and Ag-ZnO photocatalysts were prepared via a solvothermal method to photooxidize 4CP under different pH solutions. This study aims to investigate the photooxidation of 4CP at various pH solutions. At different pH levels, 4CP can exist as a parent molecule and anionic 4CP molecules. As of now, there has been no report on the photooxidation of anionic 4CP available in the literature.

■ EXPERIMENTAL SECTION

Materials

In preparing the ZnO and Ag/ZnO photocatalysts, zinc acetate dihydrate (99%, Merck, Germany) and silver nitrate (99.5%, Bendosen, Norway) were used as starting materials with isopropanol (98%, Merck, Germany) as the solvent. A stock solution of 4CP (98%, Fluka Chimie, Switzerland), prepared by dissolving 1.0 g of 4CP in 1.0 L deionized water, was diluted to produce the working solutions for the photooxidation studies. HCl and NaOH solutions were added to the 4CP working solution to adjust its pH (pH 6) to the desired pH values.

Instrumentation

A box furnace (Carbolite, USA) is used to prepare the catalyst. Powder X-ray diffractometer (X'pert Pro PanAnalytical, Philips), Belsorp Mini I Surface Area

Analyzer, Perkin Elmer Lambda 35 UV-Vis-NIR, and LS 55 Perkin Elmer fluorescence spectrophotometer were used to characterize the catalyst. A custom-made photo-reactor with a volume capacity of 1.2 L (Fig. 1) is used in the photocatalytic oxidation experiment. Perkin Elmer Lambda 35 UV-Vis-NIR was also used to determine the concentration of 4CP solution.

Procedure

Preparation of ZnO and Ag-ZnO photocatalysts

In preparing Ag-ZnO photocatalyst, a homogeneous solution containing 0.0–0.27 g of silver nitrate (0 to 2.0 mol), 14.70 g of zinc acetate dihydrate and 200 mL of isopropanol was prepared and sonicated for 1 h. The solution was placed into stainless steel autoclaves and heated at 150 °C for 3 h. The precipitate formed was collected via centrifugation, washed twice with ethanol, oven-dried at 80 °C for 24 h, and calcined at 300 °C for 2 h. A similar procedure was employed to synthesize ZnO particles.

Catalysts characterization

The XRD pattern of the photocatalysts was recorded at $2\theta = 2-60^\circ$ using a powder X-ray diffractometer (CuK α radiation at $\lambda = 1.540 \text{ \AA}$, 30 kV, and 30 mA) at the scanning rate of 2°/min. The surface area was measured by nitrogen adsorption at -196 °C using the Belsorp mini I instrument. The UV diffuse-reflectance spectrum was recorded using Perkin Elmer

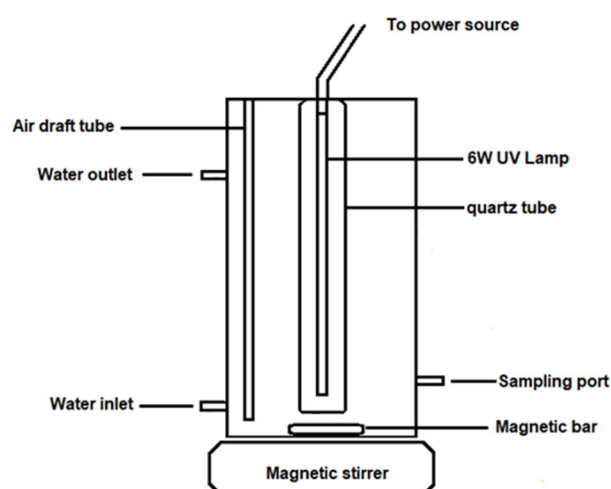


Fig 1. The schematic diagram of the photocatalytic reactor

Lambda 35 UV-Vis-NIR spectrophotometer and used to determine the bandgap energy of the photocatalysts. The electron-hole recombination was analyzed by LS 55 Perkin Elmer fluorescence spectrophotometer (PL) with an excitation wavelength set at 300 nm. A field emission-scanning electron microscope (Hitachi SU 8000) was used to capture the morphology of the photocatalyst.

Photocatalytic activity test

The photocatalytic degradation experiments were conducted using a custom-made photo-reactor equipped with water circulation to keep its temperature at 28 °C. A certain amount of catalyst ranging from 0.2 to 1.0 g was added into the photoreactor, containing a 1 L 4CP solution of known concentration ranging from 1.56×10^{-4} to 2.3×10^{-4} mol/L. After stirring the reaction mixture in the dark for 30 min to achieve adsorption-desorption equilibrium, the 6 W UV-A lamp (365 nm, Hitachi) was switched on to irradiate the solution for 240 min under a continuous supply of air. At regular intervals, 10 mL of sample were withdrawn from the bulk solution and filtered through a 0.45 μm cellulose nitrate filter to remove the catalysts. The residual concentration of 4CP during the photocatalytic oxidation experiments at solution pH of 4–9 and pH 11 was determined at λ_{max} of 225 nm and 244 nm,

respectively, using a UV-Vis spectrophotometer. The percentage of 4CP photocatalytic oxidation (PCO) was calculated as follows (Eq. (1)):

$$4\text{CP PCO (\%)} = \frac{C_o - C_t}{C_o} \times 100\% \quad (1)$$

where C_o and C_t are the concentration of 4CP initially and at time t , respectively.

RESULTS AND DISCUSSION

Catalyst Characterization

The XRD patterns of the prepared photocatalysts, shown in Fig 2, displayed a diffraction pattern matching the wurtzite structure of zinc oxide (JCPDS 036-1451). Besides, diffraction peaks observed at $2\theta = 38.1$ and 44.3° at Ag loading of 0.6 % corresponded to Ag (JCPDS 4-0783). Close examination of the XRD pattern (Fig. 2(b)) showed no significant shift in peak positions, which indicates the segregation of Ag particles in the grain boundaries of ZnO and may have formed interstitial as a second phase clusters around the ZnO lattices [25-26]. Furthermore, the Ag^+ ions cannot substitute the Zn^{2+} ions in the crystal lattice due to the difference in the oxidation states and ionic radius ($r(\text{Ag}^+) = 0.126$ nm, $r(\text{Zn}^{2+}) = 0.076$ nm) [27].

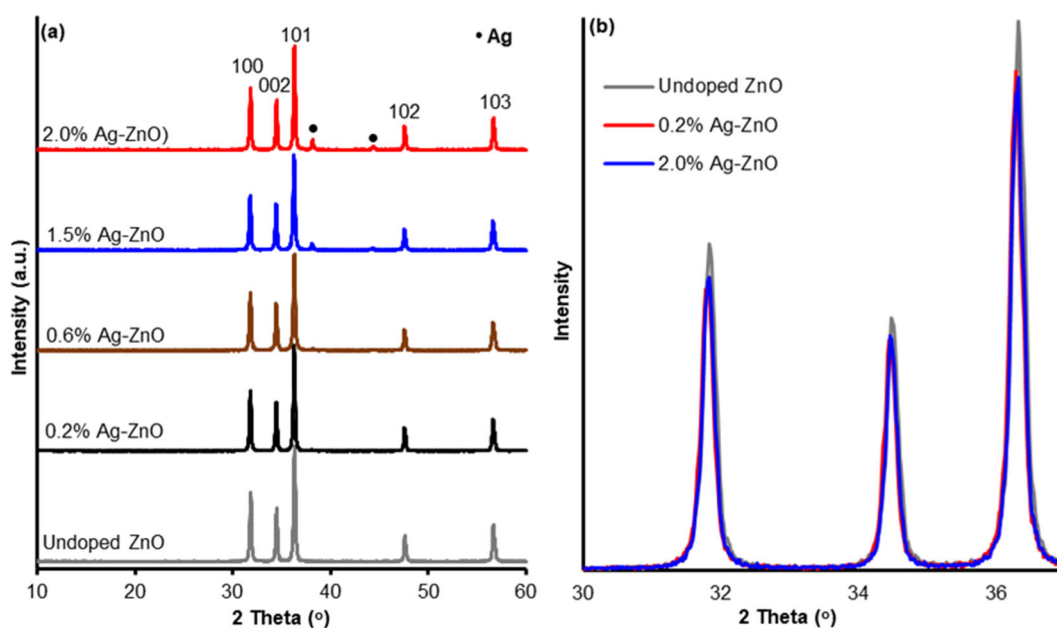


Fig 2. X-ray diffraction pattern of (a) ZnO and Ag-ZnO photocatalysts and (b) comparison of (100), (002), and (101) peaks for ZnO, 0.2% Ag-ZnO and 2.0% Ag-ZnO

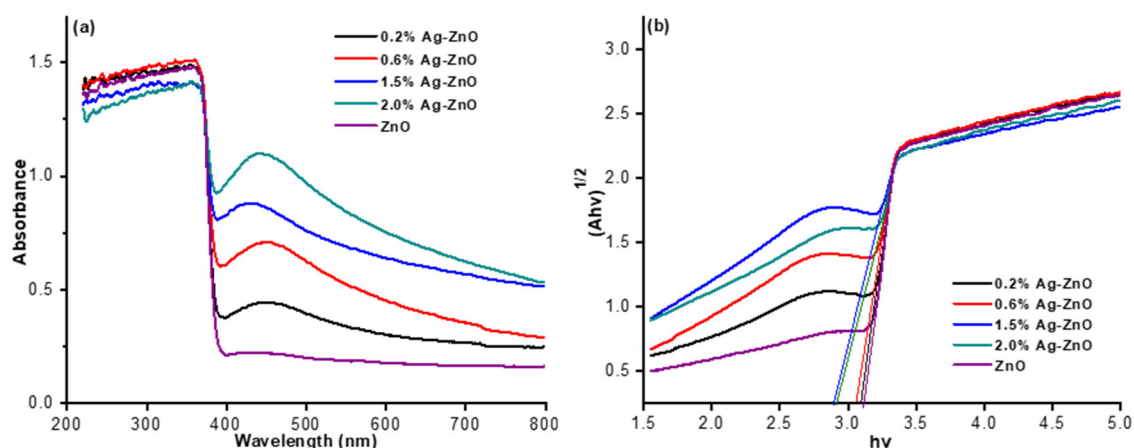


Fig 3. (a) UV-Vis spectra and (b) Tauc plot for determination of bandgap energy of ZnO and Ag-ZnO photocatalysts

The bandgap energy and surface area play an influential role in the photocatalytic activity of a photocatalyst [28]. Fig. 3 displays the UV-vis diffuse reflectance spectra and the Tauc's plot of the photocatalysts. The Ag surface plasmon resonance peak was observed at about 470 nm [29]. The peak intensity increases with the increase of Ag content, confirming that Ag has been successfully deposited on the surface of ZnO. The photocatalyst's bandgap energy, estimated from the intercept of the x-axis of the $(Ah\nu)^{1/2}$ versus $h\nu$ plot, are listed in Table 1. The addition of silver shifted the bandgap energy to 2.84 eV, changing the catalyst's optical properties from UV-activated to visible light-activated catalyst. However, the surface area of the photocatalysts was not affected by the addition of silver.

The photoluminescence (PL) study was conducted to identify the transfer, separation, and recombination of photogenerated electron-hole pairs of ZnO and Ag-ZnO. Lower PL intensity indicates a lower recombination rate of charge carriers, leading to higher photocatalytic activity. The PL spectra of ZnO and Ag-loaded ZnO are depicted in Fig. 4. Pure ZnO exhibited two emission bands at 380 nm and 420 nm. The former was attributed to the ultraviolet emission of the ZnO particles, while the latter is due to the charge carrier relaxation through the surface-related trap states [30]. As the amount of Ag increased, the PL intensity decreased significantly. The efficient interfacial charge transfer from ZnO to Ag acts as an electron sink that enhances the lifetime of the

Table 1. Surface area and bandgap energy of ZnO and Ag-ZnO photocatalysts

Photocatalyst	Surface area (m^2g^{-1})	Bandgap energy (eV)
ZnO	6.54	3.12
0.2% Ag-ZnO	6.49	3.04
0.6% Ag-ZnO	8.65	3.00
1.5% Ag-ZnO	7.71	2.84
2.0% Ag-ZnO	6.51	2.85

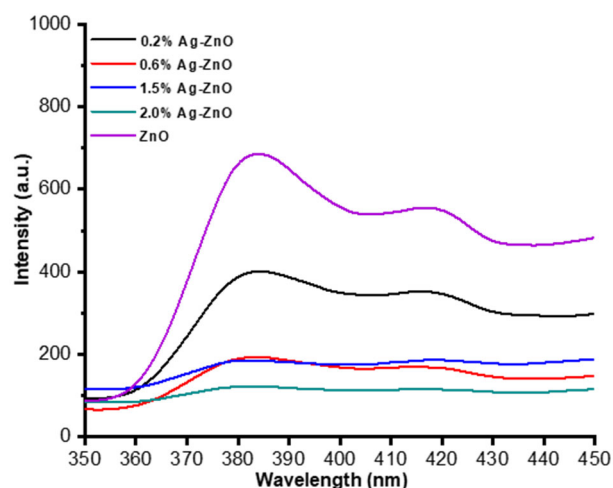


Fig 4. PL spectra of ZnO and Ag-ZnO photocatalysts

photogenerated charge carriers [31]. The morphology of the photocatalysts, depicted in Fig. 5, changed with the addition of Ag into ZnO from irregularly shaped particles (ZnO) to rod-like particles (2% Ag-ZnO). The morphological changes showed that the crystal growth of the photocatalyst is affected by the presence of Ag.

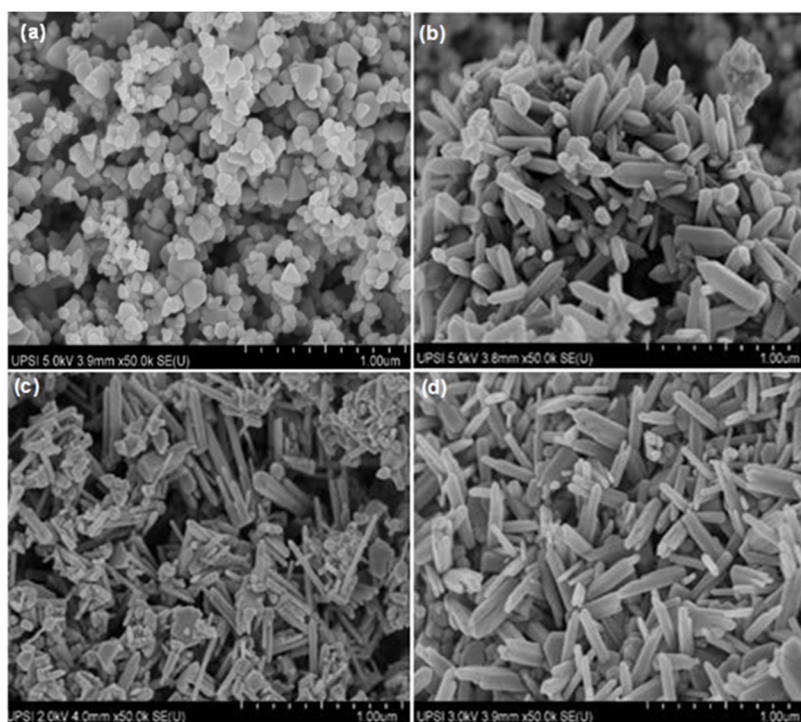


Fig 5. Micrographs of (a) ZnO (b) 0.2% (c) 0.6% (d) 2.0% Ag-ZnO photocatalysts

Photocatalytic Oxidation Activity

Fig. 6 shows the performance of ZnO and Ag-ZnO photocatalyst in the photocatalytic oxidation of 4CP. The percentage of 4CP photocatalytic oxidation increased with increasing Ag content up to 0.6% but then decreased at higher Ag content, indicating the optimum Ag loading of 0.6%. The improvement in the photocatalytic oxidation

of 4CP was due to the capability of the Ag to trap the photogenerated electron hence a better charge separation for Ag-ZnO than pure ZnO. However, excessive silver may act as recombination centers and filters that reduce the light from reaching the ZnO surface, consequently decreasing the photogeneration of charge carriers [32].

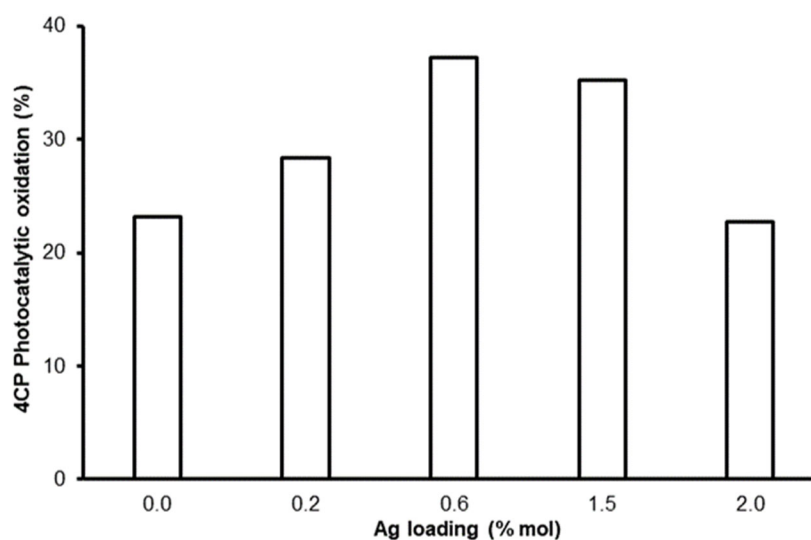


Fig 6. Photo-oxidation of 4CP by ZnO and Ag-ZnO photocatalysts (Conditions: 0.2 g photocatalysts, 1.94×10^{-4} mol/L 4CP, pH 6.0)

The influence of the mass of 0.6% Ag-ZnO photocatalyst on photo-oxidation of 4CP is shown in Fig. 7. The efficiency of the photo-oxidation increases with increasing mass up to 0.8 g (97.12%) and then decreases at a higher mass. Increasing the mass of the photocatalyst will increase photocatalytic sites, thus enhancing the photogeneration of electron and hole pairs. Consequently, more hydroxyl and superoxide radicals are produced, leading to higher photo-oxidation of 4CP [33]. However, when the mass of photocatalyst is higher than

0.8 g, the solution becomes turbid, thus reducing the light penetration into the solution, subsequently reducing the photo-oxidation of the 4CP.

The photocatalytic oxidation of 4CP, at various solution pHs, is affected by the surface charge and the stability of the catalyst, and the form of the 4CP molecule. The UV-Vis spectra of 4CP solution at different initial pH were recorded (Fig. 8) before performing the photocatalytic oxidation studies. Two peaks observed at λ_{\max} of 225 and 280 nm showed the 4CP

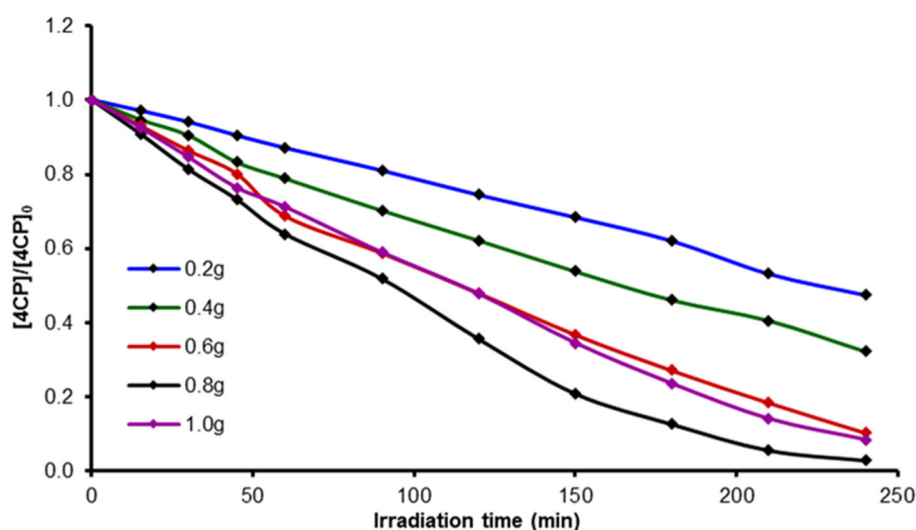


Fig 7. Photo-oxidation of 4CP by various amount of 0.6% Ag-ZnO photocatalyst (Conditions: 1.56×10^{-4} mol/L 4CP, pH 6.0)

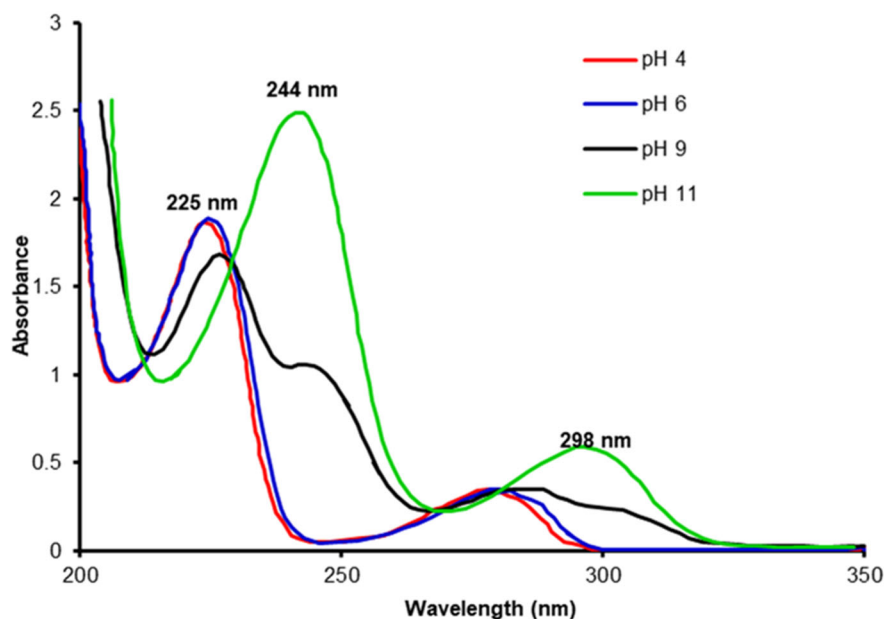


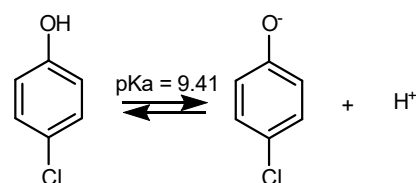
Fig 8. UV-Vis absorption spectra of 4CP with different pH solution

in its molecular form under acidic and near-neutral conditions (pH 4 and 6).

When the pH of the solution increased to 9, the 225 nm peak intensity decreased while the 280 nm peak became broader and red-shifted to 287 nm. Moreover, two shoulders appeared at 244 and 298 nm, showing partial dissociation of 4CP to its anionic form. The UV-Vis spectrum of 4CP at pH 11 displayed only the peaks at 244 and 298 nm, indicating that 4CP has completely dissociated from its anionic form [34]. These observations follow the pKa of 4CP, which is 9.4 (Scheme 1). Thus, the concentration of 4CP during the photocatalytic oxidation experiments at solution pH of 4-9 and pH 11 was then determined at λ_{\max} of 225 and 244 nm, respectively.

The photocatalytic oxidation of the 4CP molecule is also dependent on the surface charge of the catalyst. The pH of the point of zero-charge (pH_{pzc}) of the Ag-ZnO catalyst, as determined by the pH drift method [35], was 7.15. Hence, the Ag-ZnO surface is positively and negatively charged at pH below and above 7.15, respectively. The effect of the initial pH solution, ranging from pH 4 to 11, on the photocatalytic oxidation of 4CP is shown in Fig. 9. The photocatalytic oxidation increased up to pH 6, decreased slightly at pH 9, then increased significantly at pH 11. The lowest photocatalytic oxidation of 4CP, was observed at pH 4.

The progress of the 4CP photocatalytic oxidation at pH 6 to 11 is shown in Fig. 10. A steady decrease in the band intensity reflected the photocatalytic oxidation of 4CP. In the acidic and near-neutral conditions, the interaction between the positively charged Ag-ZnO and the p electron of the 4CP molecule may facilitate the photocatalytic oxidation of 4CP. At pH 9, the initial spectra of 4CP consist of 4 peaks at 225, 244 (shoulder), 287, and 298 (shoulder) nm. After the adsorption process, the 244 and 298 nm peaks were slightly visible, while the 225 nm peak became more intense. The pH of the solution also changed to 7. These changes indicate that the acidic site of the Ag-ZnO catalyst may have reacted with the added OH^- . Hence, it reduces the solution pH and causes some of the anionic 4CP molecules to return to their molecular form. The loss of acidic sites may have contributed to a slight decrease in photocatalytic oxidation of 4CP. However, at pH 11, complete photocatalytic oxidation of 4CP was observed



Scheme 1. Dissociation of 4CP and its corresponding pKa value

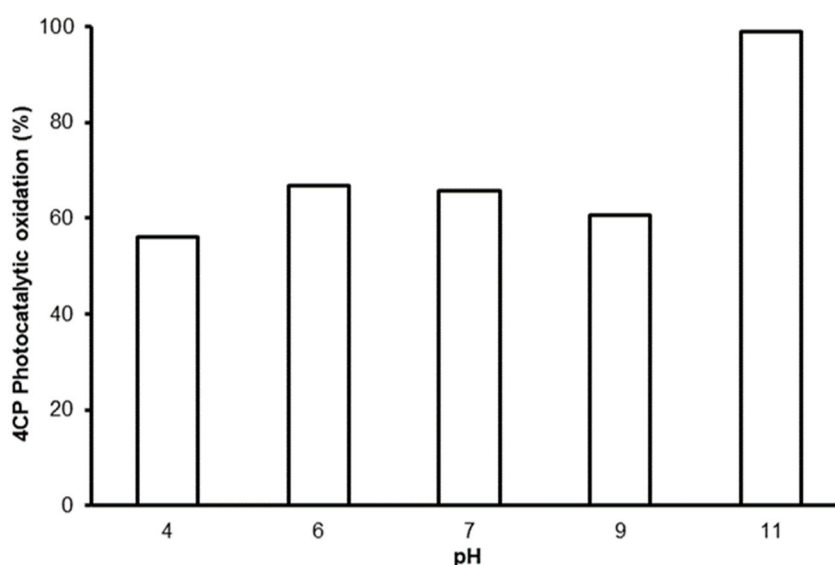


Fig 9. Photo-oxidation of 4CP under different pH of initial solution (Condition: 2.3×10^{-4} mol/L 4CP, 0.8 g of 0.6% Ag-ZnO photocatalyst)

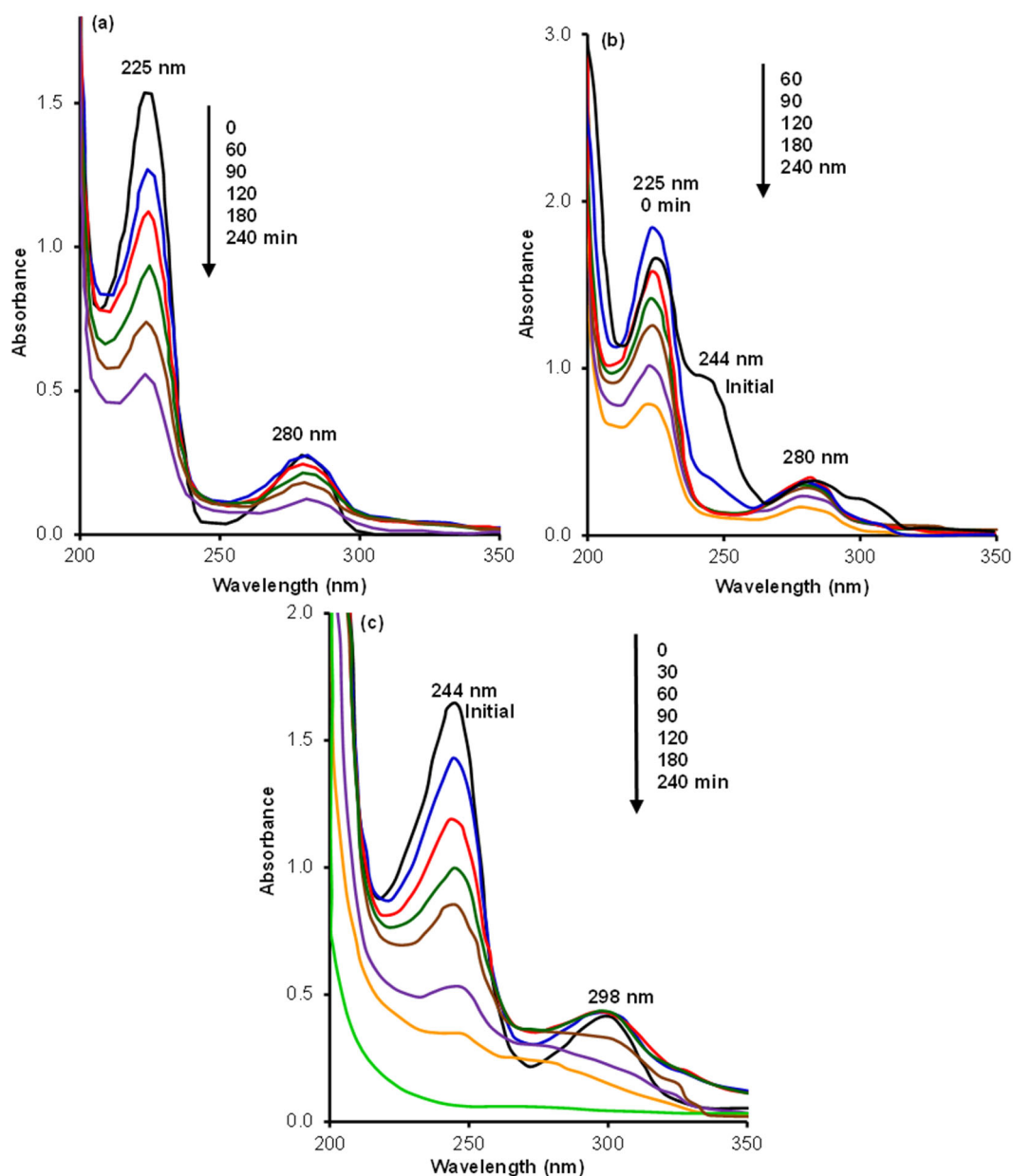


Fig 10. Progressive photo-oxidation of 4CP at (a) pH 6, (b) pH 9 and (c) pH 11

after 240 min of reaction. Theoretically, a reduction in photocatalytic oxidation of 4CP is expected in basic conditions. The reduction is due to (i) repulsion between the 4CP anion with the negatively charged surface of the catalyst and (ii) reduction in the formation of hydroxyl radicals, which is due to the competitive reaction between the hole (h^+) with the 4CP anion, H_2O and OH^- . Photolysis experiments were conducted at pH 6 and 11 to confirm that the photo-oxidation of 4CP is due to the photocatalytic reaction. The results showed that the

molecular 4CP was stable towards photolysis at pH 6, while 25% of the anionic 4CP photolyzed at pH 11. Thus, the photo-oxidation of anionic 4CP at pH 11 is due to both photolysis and photocatalytic activity.

The experimental data, fitted to the Langmuir-Hinshelwood kinetic model (Fig. 11), showed that the photocatalytic oxidation of 4CP followed the pseudo-first-order reaction. The apparent rate constants, k_{app} , were determined from the slope of the plot and are shown in the inset. The photocatalytic oxidation rate of the 4CP

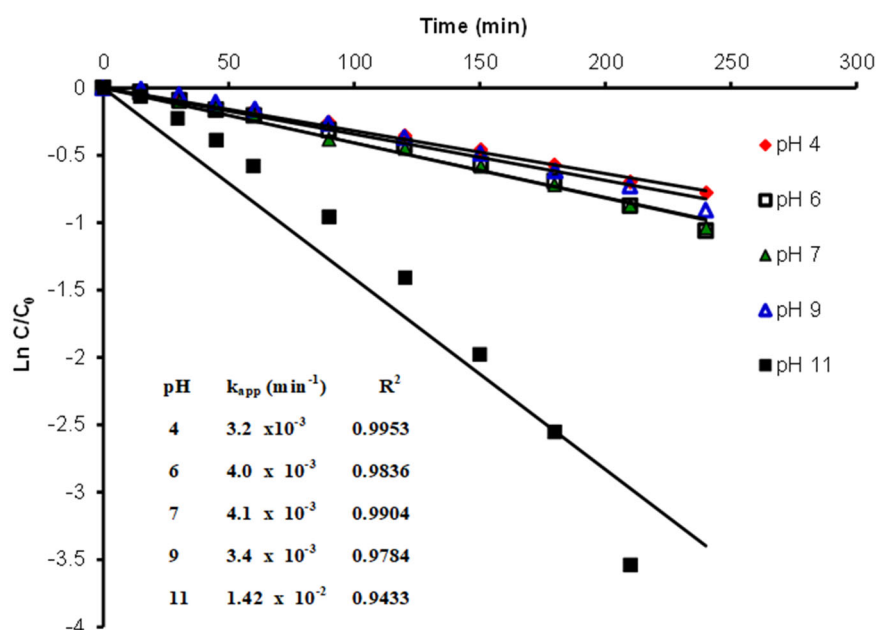


Fig 11. First-order kinetic for photo-oxidation of 4CP at different pH and its corresponding rate constant (inset)

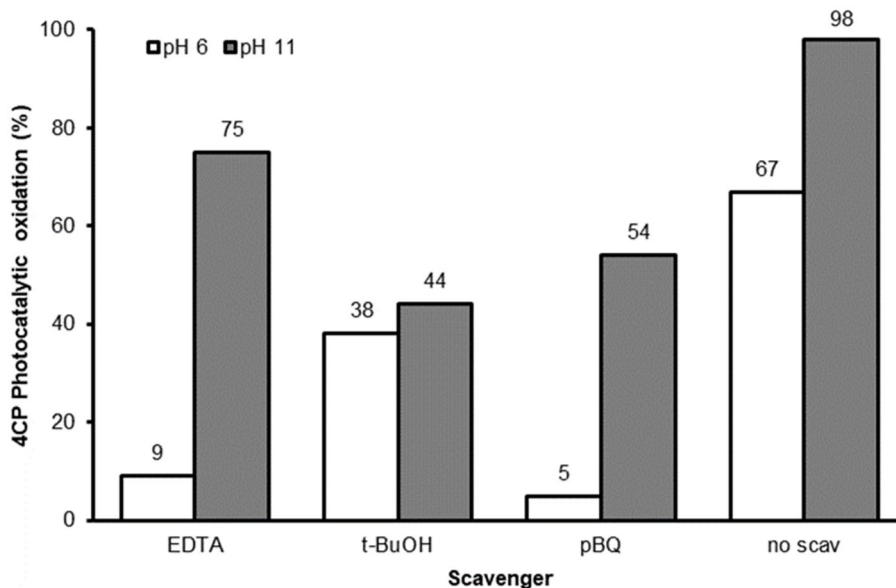


Fig 12. The effect of radical scavengers on 4CP oxidation at pH 6 and 11

molecule increased with increasing pH up to pH 6 and then decreased slightly at pH 9. The photo-oxidation rate of the anionic 4CP is approximately 4 times faster than that of molecular 4CP. Hence, the anionic 4CP is more reactive than the molecular 4CP towards photo-oxidation.

The effect of radical and hole scavengers in photocatalytic activity was conducted at pH 6 and 11 to determine the reactive species responsible for the photooxidation of 4-CP, and the results are shown in Fig.

12. Tert-butanol (t-BuOH) was used as scavengers for hydroxyl radical ($\bullet\text{OH}$), p-benzoquinone (BQ) for superoxide radical ($\bullet\text{O}_2^-$), and EDTA sodium (Na-EDTA) for the hole (h^+). The degradation of 4-CP without any scavengers was 67% at pH 6 and 98% at pH 11. At pH 6, the addition of BQ and Na-EDTA scavengers led to a significant decrease in the photooxidation of 4-CP compared to the addition of t-BuOH, indicating that both the $\bullet\text{O}_2^-$ and h^+ are the main

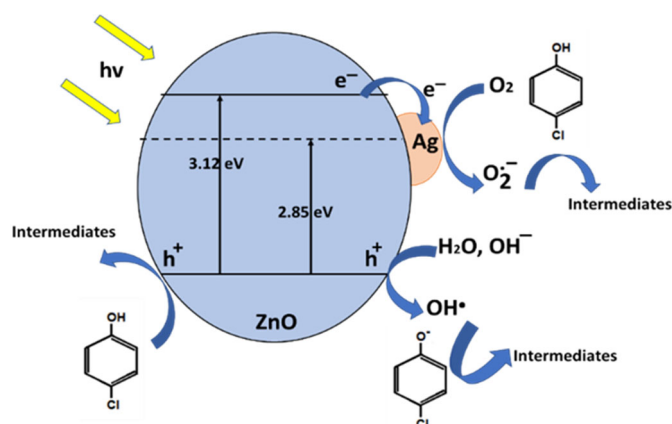


Fig 13. Proposed reaction mechanism for the photo-oxidation of molecular and anionic 4CP over Ag-ZnO catalyst

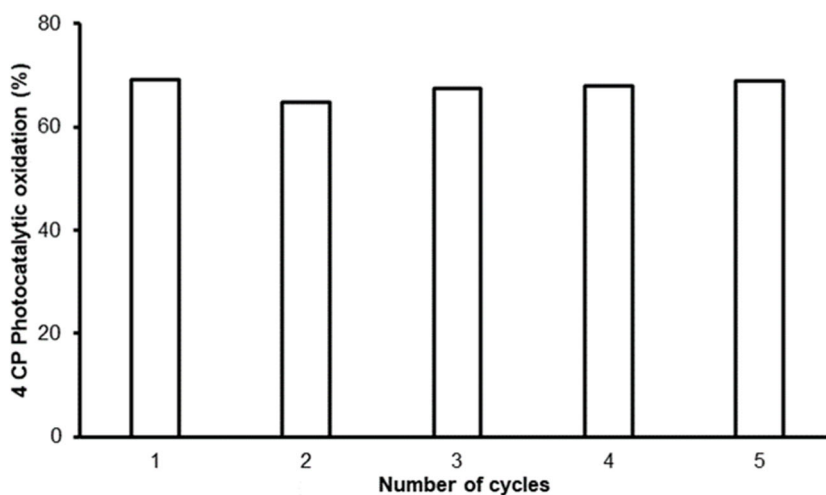


Fig 14. Reusability of 0.6% Ag-ZnO in photocatalytic oxidation of 4CP (Condition: 0.8 g photocatalyst, 2.3×10^{-4} mol/L 4CP, pH 6)

reactive species involved in the reaction system. However, a different pattern can be seen at pH 11. The photooxidation of anionic 4CP became less efficient in the presence of t-BuOH and BQ scavengers than Na-EDTA, suggesting that the $\bullet\text{OH}$ and $\bullet\text{O}_2^-$ are the active species in the reaction at pH 11. The photodegradation reaction mechanism route for molecular and anionic 4CP is different. As illustrated in Fig. 13, the photo-oxidation of molecular 4CP proceeded via reaction with the holes and superoxide radicals, while photooxidation of anionic 4CP occurs via reaction with hydroxyl radicals.

Reusability

The reusability test of the photocatalyst was investigated at optimum photo-oxidation conditions i.e.

0.8 g of 0.6% Ag-ZnO catalyst, 2.3×10^{-4} mol/L 4CP solution at natural pH (pH 6). At the end of the experiment, the catalyst was recovered by filtration, washed with deionized water, and then used to degrade a fresh 4CP solution. As shown in Fig. 14, no significant difference in the percentage of 4CP photo-oxidation was observed up to 5 cycles of photo-oxidation experiment, thus indicating the Ag-ZnO photocatalyst's stability during the photo-oxidation of the 4CP molecules.

CONCLUSION

ZnO and Ag-ZnO photocatalysts with hexagonal wurtzite ZnO structures were successfully synthesized under mild solvothermal conditions. The performance of ZnO in the photocatalytic oxidation of 4CP was

enhanced by the presence of Ag, with 0.6% Ag-ZnO exhibiting the highest photocatalytic activity. The photocatalytic oxidation of 4CP is affected by the pH of the 4CP solution. Approximately 68% of molecular 4Cp was photo oxidized at pH 6, while a nearly complete photo-oxidation of anionic 4CP was observed at pH 11 when oxidizing 2.3×10^{-4} mol/L 4CP using 0.8 g catalyst, indicating a higher reactivity of the anionic 4CP towards photolysis and photocatalysis. The photocatalytic oxidation of 4CP followed the Langmuir-Hinshelwood first-order kinetic model. The stability and the reusability studies showed that the prepared Ag/ZnO photocatalyst has good potential to efficiently oxidize molecular and anionic 4CP in acidic and alkaline conditions, hence can be used to photo-oxidize other chlorophenol compounds.

■ ACKNOWLEDGMENTS

The authors also acknowledged the Ministry of Higher Education, Malaysia, for the financial assistance under grant project FRGS/FASA1-2011/(SG)/(UPM)/(02/38) and MyBrain Scholarship to NSHR, respectively. The authors also acknowledged the Faculty of Science, and Institute of Advanced Technology, Universiti Putra Malaysia, for providing the research facilities.

■ AUTHOR CONTRIBUTIONS

Abdul Halim Abdullah, Mohd Izham Saiman, Lee Kian Mun and Nur Syafiq Hazirah Razali proposed and designed the project. Nur Syafiq Hazirah Razali and Hayati Mukhair conducted the experiments and write the original draft. Abdul Halim Abdullah, Nur Syafiq Hazirah Razali and Hayati Mukhair analyzed and validated the data. Abdul Halim Abdullah, Mohd Izham Saiman, Lee Kian Mun reviewed and revised the manuscript. All authors agreed to the final version of this manuscript.

■ REFERENCES

- [1] Castañeda, C., Tzompantzi, F., Gómez, R., and Rojas, H., 2016, Enhanced photocatalytic degradation of 4-chlorophenol and 2,4-dichlorophenol on in situ phosphated sol-gel TiO₂, *J. Chem. Technol. Biotechnol.*, 91 (8), 2170–2178.
- [2] Lavand, A.B., and Malghe, Y.S., 2015, Visible light photocatalytic degradation of 4-chlorophenol using C/ZnO/CdS nanocomposite, *J. Saudi Chem. Soc.*, 19 (5), 471–478.
- [3] Mahrouqi, H.K.N., Nawi, M.A., and Nawawi, W.I., 2014, Photodegradation of 4-chlorophenol using carbon coated TiO₂ under solar irradiation, *Int. J. Sci. Res. Publ.*, 4 (6), 1–7.
- [4] Munshi, G.H., Ibrahim, A.M., and Al-Harbi, L.M., 2018, Inspired preparation of zinc oxide nanocatalyst and the photocatalytic activity in the treatment of methyl orange dye and paraquat herbicide, *Int. J. Photoenergy*, 2018, 5094741.
- [5] Li, L., Sun, S.Q., Wang, Y.X., and Wang, C.Y., 2018, Facile synthesis of ZnO/g-C₃N₄ composites with honeycomb-like structure by H₂ bubble templates and their enhanced visible light photocatalytic performance, *J. Photochem. Photobiol., A*, 355, 16–24.
- [6] Mendoza-Mendoza, E., Nuñez-Briones, A.G., García-Cerda, L.A., Peralta-Rodríguez, R.D., and Montes-Luna, A.J., 2018, One-step synthesis of ZnO and Ag/ZnO heterostructures and their photocatalytic activity, *Ceram. Int.*, 44 (6), 6176–6180.
- [7] Kavitha, R., and Kumar, S.G., 2019, A review on plasmonic Au-ZnO heterojunction photocatalysts: Preparation, modifications and related charge carrier dynamics, *Mater. Sci. Semicond. Process.*, 93, 59–91.
- [8] Jefri, S.N.S., Abdullah, A.H., and Muhamad, E.N., 2019, Response surface methodology: photodegradation of methyl orange by CuO/ZnO under UV light irradiation, *Asian J. Green Chem.*, 3 (2), 271–287.
- [9] He, R., Hocking, R.K., and Tsuzuki, T., 2012, Co-doped ZnO nanopowders: Location of cobalt and reduction in photocatalytic activity, *Mater. Chem. Phys.*, 132 (2-3), 1035–1040.
- [10] Ravishankar, T.N., Manjunatha, K., Ramakrishnappa, T., Nagaraju, G., Kumar, D., Sarakar, S., Anandakumar, B.S., Chandrappa, G.T., Reddy, V., and Dupont, J., 2014, Comparison of the

- photocatalytic degradation of trypan blue by undoped and silver-doped zinc oxide nanoparticles, *Mater. Sci. Semicond. Process.*, 26, 7–17.
- [11] Sopian, N.A.M., Nor, R.M., Rafaie, H.A., Sani, S.F.A., and Osman, Z., 2018, Photocatalytic degradation of methylene blue with silver doped ZnO nanoparticles grown on microscopic sand particles, *Malays. J. Anal. Sci.*, 22 (2), 270–278.
- [12] Chitradevi, T., Lenus, A.J., and Jaya, N.V., 2020, Structure, morphology and luminescence properties of sol-gel method synthesized pure and Ag-doped ZnO nanoparticles, *Mater. Res. Express*, 7, 015011.
- [13] AL-Jawad, S.M.H., Sabeeh, S.H., Taha, A.A., and Jassim, H.A., 2018, Studying structural, morphological and optical properties of nanocrystalline ZnO:Ag films prepared by sol-gel method for antimicrobial activity, *J. Sol-Gel Sci. Technol.*, 87 (2), 362–371.
- [14] Alshamsi, H.A.H., and Hussein, B.S., 2018, Hydrothermal preparation of silver doping zinc oxide nanoparticles: Study, characterization and photocatalytic activity, *Orient. J. Chem.*, 34 (4), 1898–1907.
- [15] Behera, T.K., Pradhan, S., Satapathy, P.K., and Mohapatra, P., 2021, Synthesis and characterization of ZnO-Ag plasmonic nanocomposite: An efficient photocatalyst for the degradation industrial pollutant, *Mater. Today: Proc.*, 47, 1159–1162.
- [16] Singh, R., Barman, P.B., and Sharma, D., 2017, Synthesis, structural and optical properties of Ag doped ZnO nanoparticles with enhanced photocatalytic properties by photo degradation of organic dyes, *J. Mater. Sci.: Mater. Electron.*, 28 (8), 5705–5717.
- [17] Shojaei, A.F., Tabatabaeian, K., Zanjanchi, M.A., Moafi, H.F., and Modirpanah, N., 2015, Synthesis, characterization and study of catalytic activity of silver doped ZnO nanocomposite as an efficient catalyst for selective oxidation of benzyl alcohol, *J. Chem. Sci.*, 127 (3), 481–491.
- [18] Rasaki, S.A., Zhao, C., Wang, R., Wang, J., Jiang, H., and Yang, M., 2019, Facile synthesis approach for preparation of robust and recyclable Ag/ZnO nanorods with high catalytic activity for 4-nitrophenol reduction, *Mater. Res. Bull.*, 119, 110536.
- [19] Xu, Z., Liu, N., Han, Y., Zhang, P., Hong, Z., and Li, J., 2021, Preparation of Ag/ZnO microspheres and study of their photocatalytic effect on dichloromethane, *Desalin. Water Treat.*, 216, 162–169.
- [20] Ong, C.B., Ng, L.Y., and Mohammad, A.W., 2018, A review of ZnO nanoparticles as solar photocatalysts: Synthesis, mechanisms, and applications, *Renewable Sustainable Energy Rev.*, 81 (1), 536–551.
- [21] Igbinosa, E.O., Odjadjare, E.E., Chigor, V.N., Igbinosa, I.H., Emoghene, A.O., Ekhaize, F.O., and Idemudia, O.G., 2013, Toxicological profile of chlorophenols and their derivatives in the environment: The public health perspective, *Sci. World J.*, 2013, 460215.
- [22] Byrne, C., Subramanian, G., and Pillai, S.C., 2018, Recent advances in photocatalysis for environmental applications, *J. Environ. Chem. Eng.*, 6 (3), 3531–3555.
- [23] de Moraes, N.P., Marins, L.G.P., de Moura Yamanaka, M.Y., Bacani, R., da Silva Rocha, R., and Rodrigues, L.A., 2021, Efficient photodegradation of 4-chlorophenol under solar radiation using a new ZnO/ZnS/carbon xerogel composite as a photocatalyst, *J. Photochem. Photobiol., A*, 418, 113377.
- [24] Rajendran, S., Pachaiappan, R., Hoang, T.K.A., Karthikeyan, S., Gnanasekaran, L., Vadivel, S., Soto-Moscoso, M., and Gracia-Pinilla, M.A., 2021, CuO-ZnO-PANI a lethal p-n-p combination in degradation of 4-chlorophenol under visible light, *J. Hazard. Mater.*, 416, 125989.
- [25] Welderfael, T., Yadov, O.P., Taddesse, A.M., and Kaushal, J., 2013, Synthesis, characterization and photocatalytic activities of Ag-N-codoped ZnO nanoparticles for degradation of methyl red, *Bull. Chem. Soc. Ethiop.*, 27 (2), 221–232.
- [26] Lupan, O., Chow, L., Ono, L.K., Cuenya, B.R., Chai, G., Khallaf, H., Park, S., and Schulte, A., 2010,

- Synthesis and characterization of Ag- or Sb-doped ZnO nanorods by a facile hydrothermal route, *J. Phys., Chem. C*, 114 (29), 12401–12408.
- [27] Jung, D., 2010, Syntheses and characterization of transition metal-doped ZnO, *Solid State Sci.*, 12 (4), 466–470.
- [28] Fatima, S., Ali, S.I., Iqbal, M.Z., and Rizwan, S., 2017, The high photocatalytic activity and reduced band gap energy of La and Mn co-doped BiFeO₃/graphene nanoplatelet (GNP) nanohybrids, *RSC Adv.*, 7 (57), 35928–3593.
- [29] Murali, A., Sarswat, P.K., Perez, J.P.L., and Free, M.L., 2020, Synergetic effect of surface plasmon resonance and schottky junction in Ag-AgX-ZnO-rGO (X= Cl & Br) nanocomposite for enhanced visible-light driven photocatalysis, *Colloids Surf., A*, 595, 124684.
- [30] Patil, S.S., Mali, M.G., Tamboli, M.S., Patil, D.R., Kulkarni, M.V., Yoon, H., Kim, H., Al-Deyab, S.S., Yoon, S.S., Kolekar, S.S., and Kale, B.B., 2016, Green approach for hierarchical nanostructured Ag-ZnO and their photocatalytic performance under sunlight, *Catal. Today*, 260, 126–134.
- [31] Zhang, X., Wang, Y., Hou, F., Li, H., Yang, Y., Zhang, X., Yang, Y., and Wang, Y., 2017, Effects of Ag loading on structural and photocatalytic properties of flower-like ZnO microspheres, *Appl. Surf. Sci.*, 391, 476–483.
- [32] Jia, Z., Peng, K., Li, Y., and Zhu, R., 2012, Preparation and photocatalytic performance of porous ZnO microrods loaded with Ag, *Trans. Nonferrous Met. Soc. China*, 22 (4), 873–878.
- [33] Dehdar, A., Asgari, G., Leili, M., Madrakian, T., and Seid-mohammadi, A., 2021, Step-scheme BiVO₄/WO₃ heterojunction photocatalyst under visible LED light irradiation removing 4-chlorophenol in aqueous solutions, *J. Environ. Manage.*, 297, 113338.
- [34] Matafonova, G., Philippova, N., and Batoev, V., 2011, The effect of wavelength and pH on the direct photolysis of chlorophenols by ultraviolet excilamps, *Eng. Lett.*, 19 (1), 20–23.
- [35] Kumar, T.K.M.P., Mandlimath, T.R., Sangeetha, P., Sakthivel, P., Revathi, S.K., Kumar, S.K.A., and Sahoo, S.K., 2015, Highly efficient performance of activated carbon impregnated with Ag, ZnO, and Ag/ZnO nanoparticle as antimicrobial materials, *RSC Adv.*, 5 (130), 108034–108043.